C. Lin
R. F. Sullivan

An Application of White Light Interferometry in Thin Film Measurements

Abstract: An application of the white light interferometry technique has been developed for measuring the thickness of thin films. The technique is used in the development of sliders which serve as carriers for the magnetic transducers (read/write elements) that operate in close proximity to magnetic disks. With the proper design of a surface contour and the applied load on the slider, a self-acting air bearing is created under the slider due to the boundary layer existing on a rotating disk.

To evaluate the performance of these sliders, parameters such as surface contour and steady-state slider-to-disk spacing must be determined. Since these parameters have a magnitude of only a few wavelengths of visible light, a light interference technique was chosen for their measurement. Conventionally, measurements of this kind are made with monochromatic light. However, when measurement magnitudes are less than 1 μm, the resolution of white light interferometry surpasses that of the monochromatic technique.

The white light interference pattern is a continuous color spectrum instead of the dark and bright fringes of the monochromatic technique. For a film thickness of less than 1 μm these colors can be identified to a resolution of 0.05 μm, as compared with 0.15 to 0.20 μm for the visible monochromatic fringes of the technique currently applied to the measurement of these parameters.

Introduction

Self-acting air-lubricated slider bearings have been used successfully in the computer industry for the past ten years. One purpose of the slider is to provide the structural support for a core (magnetic transducer) and a means for positioning and maintaining the core in close proximity to a magnetic disk during the recording process. Figure 1 shows the configuration of the self-acting slider on a recording disk.

The slider maintains a self-acting (sometimes called hydrodynamic) lubricating film between the slider and the moving disk surface. This film develops a load-carrying capacity due to a wedge effect. The behavior of this lubricating film is governed by the Reynolds equation with the proper boundary conditions. For a theoretical analysis and design of self-acting sliders, refer to Gross [1] and Tang [2]. The four basic, commonly used slider configurations are the plane wedge, the step, the tapered flat, and the cylindrical curve (see Fig. 2).

One of the major evolutions in magnetic recording has been the continuous effort to achieve higher recording bit densities. The relationship between spacing and recording bit density has been illustrated in various texts on magnetic recording [3]. Generally, an increase in bit density requires a decrease in spacing. Over the years slider-to-disk spacing has dropped from 6 to less than 1 μm. Evaluation of the sliders at spacings within the range of 1 to 6 μm, using monochromatic light, has been described by Lieskovsky [4]. For spacings of less than 1 μm, the white light interferometry technique presented here offers resolution surpassing that of the monochromatic technique.

Interference of light fringes with monochromatic light

To understand how the interference pattern created by a white light source is interpreted, interference in a thin film created by a monochromatic light source must be investigated. Figure 3 shows a ray of monochromatic light incident on a thin film of air. A portion of the incident light is reflected at the top boundary of the thin film (surface 1), while the remainder is refracted and transmitted through the boundary into the air film. At the lower boundary of the air film (surface 2), a portion of the transmitted light is reflected back through the film. Upon emerging from the thin film, the ray reflected from the lower boundary has an intensity comparable to that of the ray reflected from the upper boundary and the two combine to form an interference pattern. The effect of

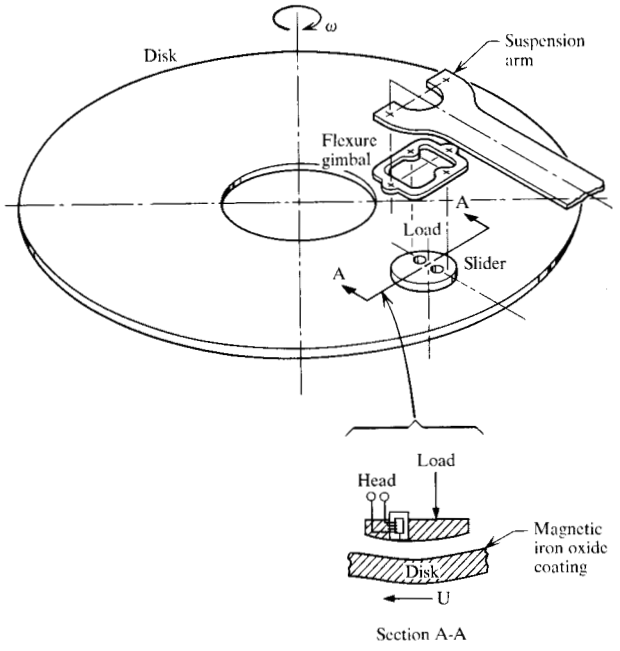

Figure 1 Configuration of a self-acting slider on a recording disk.

Figure 2 Four basic slider configurations. (a) Plane wedge; (b) step; (c) curved; (d) tapered flat.

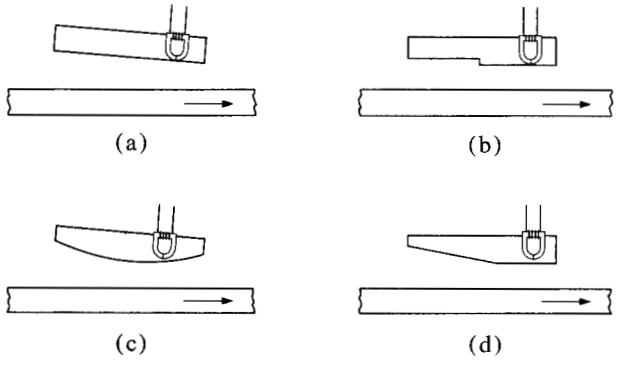

other reflected rays can be neglected because their intensity is negligible compared with that of the first two [5,6].

If the two rays are in phase, maximum reinforcement occurs, whereas if they are out of phase the reinforcement diminishes until total annihilation occurs when the phase difference is 180° ($\lambda/2$). The phase difference of the two rays is controlled by two factors: the difference in optical path length $2dn\cos\theta$ (see Fig. 3), and the phase shift of 180° ($\lambda/2$) that occurs when the light ray reflects from a more dense to a less dense medium.

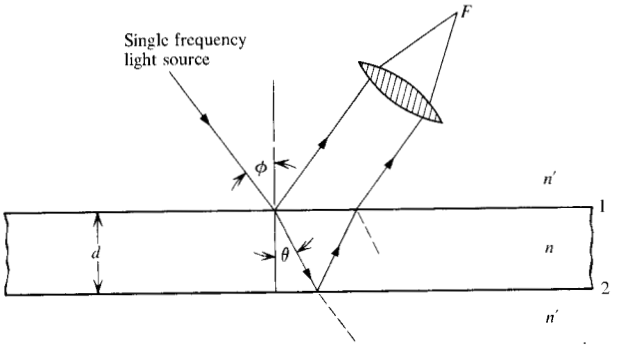

Figure 3 Optical path length difference for multiple reflection of monochromatic light.

For normal incidence ($\phi = 0$; see Fig. 3), the rays reflected from the two boundaries of the thin film interact to form an interference pattern with an intensity that can be approximated as

$$I = K \sin^2 (2\pi d/\lambda), \tag{1}$$

where λ is the wavelength of incident light in the thin film medium, d is the film thickness, and K is constant for a given film. Total reinforcement or constructive interference results in a maximum light intensity and occurs when the path length difference is

$$2d = (m + \tfrac{1}{2})\lambda, \tag{2}$$

where $m = 0,1,2, \cdots$ (maxima).

Annihilation or destructive interference, which results in a minimum light intensity, occurs when the path difference is

$$2d = m\lambda, \tag{3}$$

where $m = 0, 1, 2, \cdots$ (minima).

Therefore, as the film thickness d increases from zero, where destructive interference occurs due to the phase shift of the external reflection, the intensity increases to a maximum at a separation equal to $\lambda/4$. It then decreases until another minimum is encountered at $d = \lambda/2$, etc. These bright and dark fringes are illustrated in Fig. 4 for three frequencies in the visible spectrum. The thin film being measured is an air wedge created by loading a slider against an optical flat. The zero fringe order is at the bottom of each photograph, with the maximum film thickness at the top. The fringe order at any point in the thin film is dependent upon the wavelength of the incident light. This is illustrated in Fig. 4 by the fact that for the same air-film thickness there are seven fringes for 6250-Å red light, eight fringes for 5500-Å green light, and nine fringes for 5000-Å blue light. The light source for these monochromatic frequencies was a tunable monochromator.

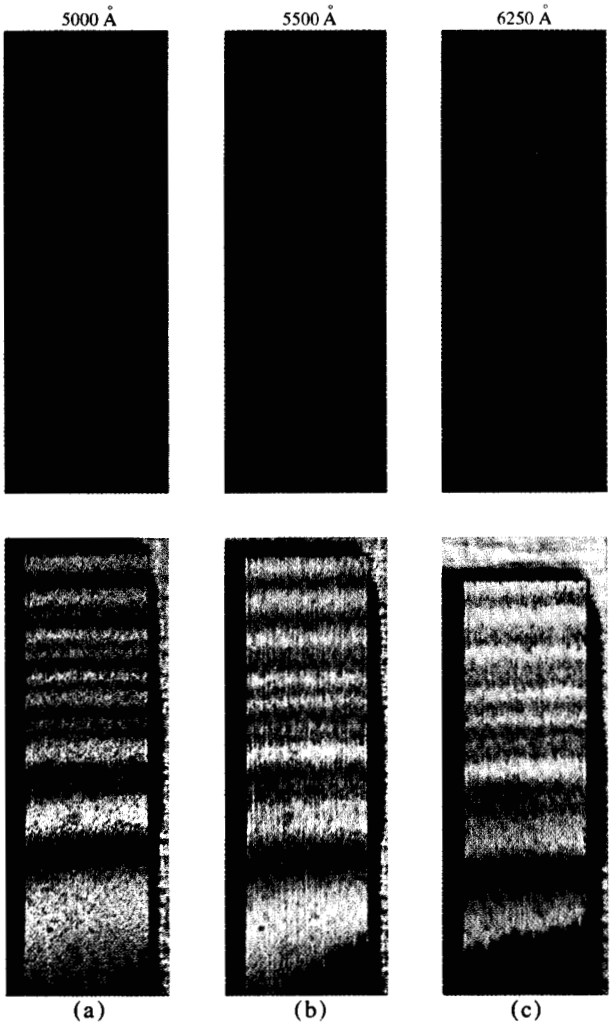

Figure 4 Interference patterns of thin air film. Top: three monochromatic light sources. Bottom: (a) superposition of the three monochromatic light sources above; (b) superposition of all wavelengths in visible spectrum; (c) tungsten filament lamp with a color correction filter.

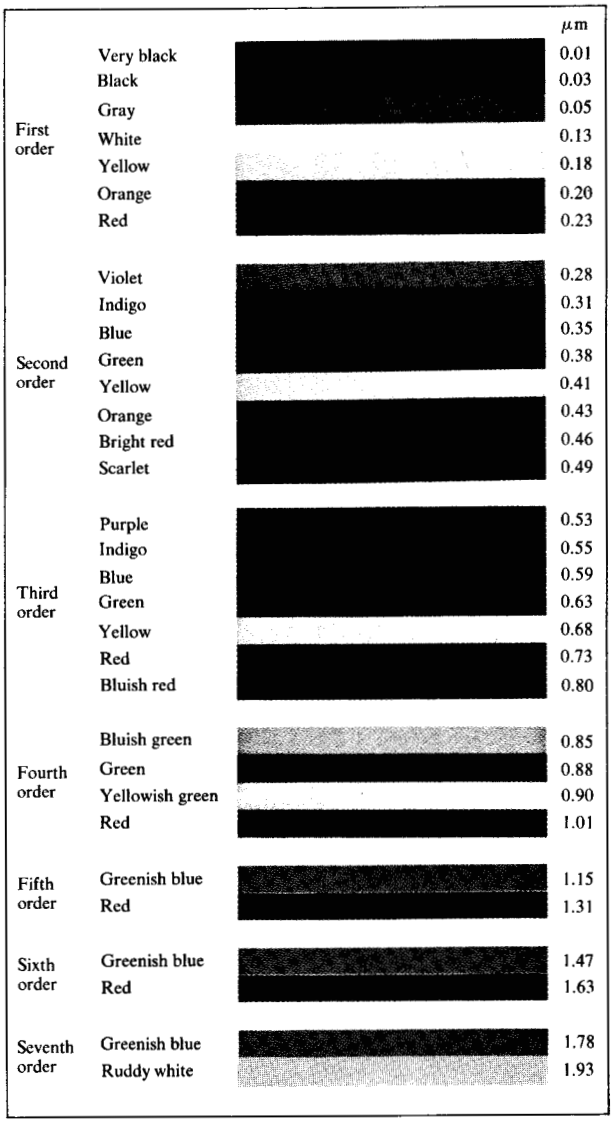

Figure 5 Newton's color scale.

Interference of light fringes with white light

With a white light source, the interference pattern from a thin film consists of a continuous color spectrum instead of the dark and bright fringes of the monochromatic pattern. As illustrated by the monochromatic photographs in Fig. 4, each wavelength forms its own interference pattern. Therefore, for white light illumination, the color of the interference pattern at any point in the thin film is due to the superposition of those colors whose wavelength intensities are strengthened through constructive interference and the absence of those colors whose wavelength intensities are weakened due to destructive interference at that particular film thickness [6,7].

An artist's rendition of the colors resulting from the white light interference phenomenon is depicted in Newton's Color Scale, Fig. 5. The color designations and corresponding film thicknesses are those that Newton set forth in his *Opticks* [6]. The color scale is separated into fringe orders at the transition from red to blue or green because these points are readily identified and quite useful in using the chart.

Generally, white light fringes are observable only up through the sixth or seventh fringe orders (1.75 to 2 μm). Also, as the fringe order increases, the resolution of the technique decreases. The most useful operating range is from zero to the third or fourth fringe order (0 to 1 μm). In this range the resolution is approximately 0.05 μm. This can be seen in Fig. 5, where the second order yellow represents a film thickness of 0.4 μm and second order red is 0.45 μm. Therefore, a 0.05 μm difference

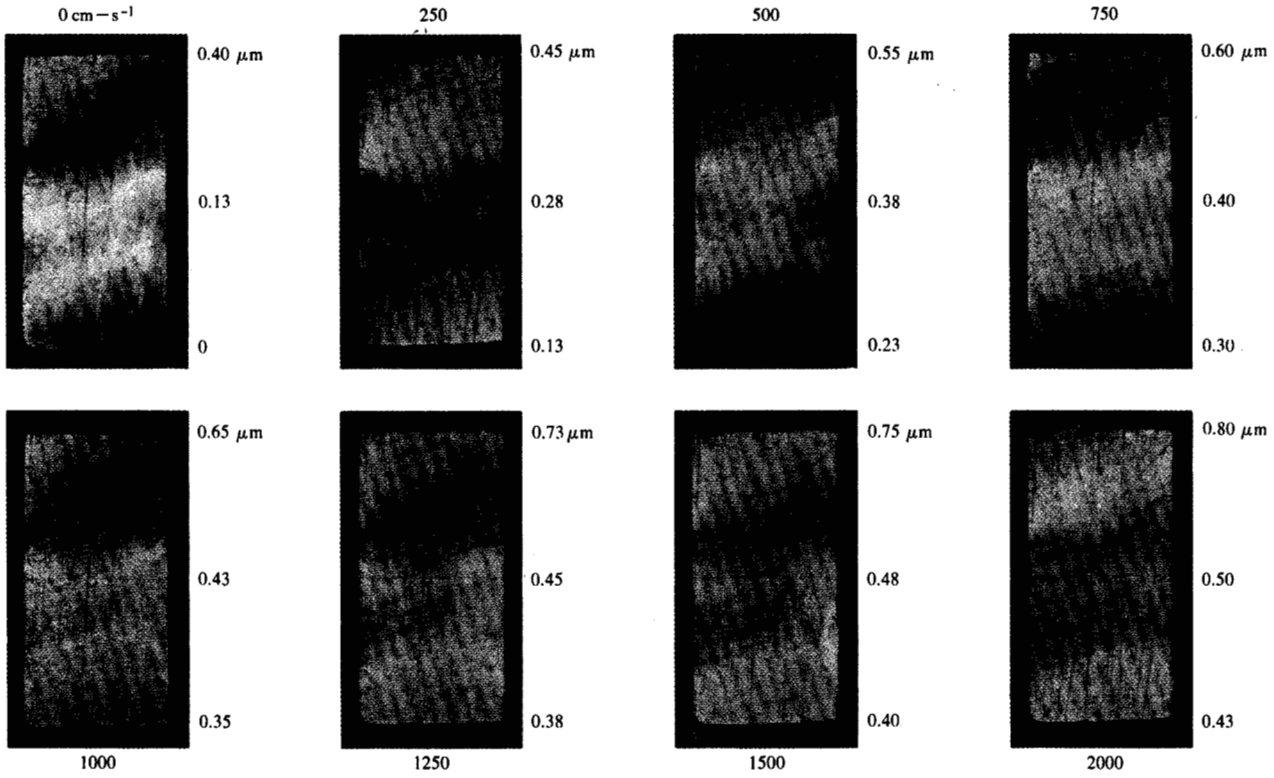

Figure 6 Color changes vs speed for ceramic slider on glass disk, viewed through disk. Speed is shown above or below each photograph. Numerical values for spacing are superimposed on the photographs at the locations of the corresponding color bands.

can easily be distinguished. The zero order can be established quite readily since it contains the only black fringe on the color scale. This black fringe results from the destructive interference of all wavelengths at zero film thickness.

The film thickness for which white light interferometry is effective is limited, because the fringes are distinct only if the film thickness is not much greater than the wavelength of the incident light [7–9]. This is best understood by examining the expression for the path length difference at which maximum intensity occurs, $2d = (m + \frac{1}{2})\lambda$. For any film thickness from zero to 0.5 μm, only a single wavelength in the visible spectrum gains maximum intensity. The colors are quite pure and distinct, except from 0 to 0.15 μm. Here, the wavelengths in the visible spectrum reach their first intensity maximum so close together that the integrated interference pattern appears as a fringe, changing from black at zero through grey to white at 0.125 μm before the first yellow fringe appears at 0.175 μm.

From 0.5 to 1 μm there are two wavelengths in the visible spectrum that reach a maximum intensity at any given film thickness. From 1.1 to 1.5 μm, there are three such wavelengths, etc. As the number of wavelengths that reach simultaneous maxima increases, the color of the interference fringe appears less distinct, until the superposition is such that the result is practically white illumination.

Applications

White light interferometry has been used to evaluate slider parameters such as slider surface contour and steady-state slider-to-disk spacing. The technique was chosen for these applications because of its ability to produce excellent resolution in the region where most of the parameters would be measured. Other desirable features of the technique are simplicity of equipment, namely, a microscope with a built-in vertical illuminator, and the ability to make full-field permanent documentation through color photography.

• *Surface contour*

Generally, the first parameter to be inspected on a slider is the surface contour. This surface determines the air bearing characteristics for each slider, which in turn govern the slider-to-disk spacing at a given speed. The surface contour is inspected by loading the slider against an optical flat, which simulates the disk surface. The contour is then inspected through the optical flat with a microscope. Color photographs of the interference pat-

tern created by the surface contour are taken for documentation. Such photographs are similar to the zero speed photograph shown in Fig. 6, which was made with the slider in contact with the optical flat (bottom of photograph).

• *Slider-to-disk spacing*

Probably the most important application of the white light interference technique is the measurement of slider-to-disk spacing. When a slider is loaded against a rotating glass disk, which simulates the functional surface as shown in Fig. 7(a), the same interference phenomenon occurs as when a slider is loaded against an optical flat. As the rotational speed of the disk changes, the slider-to-disk spacing changes. This is observed as a change of color in the interference pattern.

These color changes are recorded by starting with the glass disk at rest to identify the zero order fringe, and then following the color and fringe orders as the disk speed is increased. Or the speed can be lowered after the slider is flying, until the slider-to-disk spacing is 0.35 μm, where a very distinctive blue fringe occurs in the second order. From this point the colors and fringe orders are monitored as the disk speed is increased to its operating value.

Examples of the color changes associated with the speed variations are illustrated in Fig. 6, with the minimum slider-to-disk spacing occurring at the bottom of the photographs. Typical results of such tests are presented in Fig. 8, where the minimum slider-to-disk spacing is plotted against disk velocity.

In addition to steady-state slider-to-disk spacing observations, dynamic stability of the slider can be observed in a qualitative manner. For very low frequency fluctuations, the human eye is usually capable of distinguishing the magnitude of the variations in the interference pattern. For higher frequency fluctuations, the interference pattern appears to be washed out because the eye integrates the color changes associated with the changes in slider-to-disk spacing. When the amplitude of the high frequency fluctuation is greater than 0.2 μm, the interference pattern is completely washed out and the color appears as a whitish grey.

To verify the relevance of this information, a slider fabricated from a transparent material has been observed on a functional surface. This setup is depicted schematically in Fig. 7(b). The verification is accomplished by measuring the slider-to-disk spacing using the transparent slider under three test conditions.

Initially, the transparent slider is flown on a glass disk and the slider-to-disk spacing is viewed through the glass disk, as is normally done with functional sliders. This situation is shown schematically in Fig. 7(a), with photographic illustrations shown in Fig. 9. Then the slider-to-

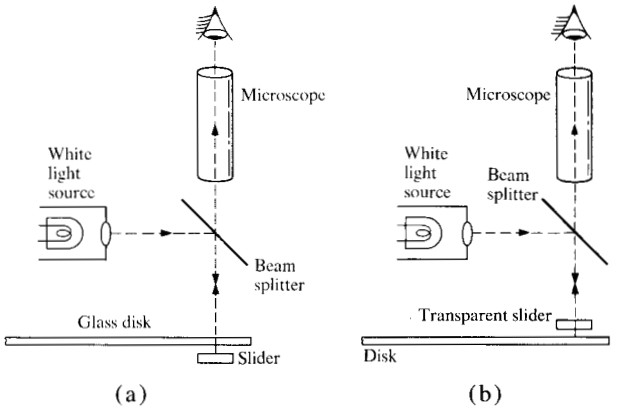

Figure 7 Schematic of techniques used to measure slider-to-disk spacing (a) through glass disk; (b) through transparent slider.

Figure 8 Minimum slider-to-disk spacing vs speed from white light interference pattern.

Observed data to be translated by Newton's color scale

Speed (cm−s^{-1})	Order	Color
0	First	Black
250	First	White
500	First	Red
750	Second	Indigo
1000	Second	Blue
1250	Second	Green
1500	Second	Yellow
2000	Second	Orange

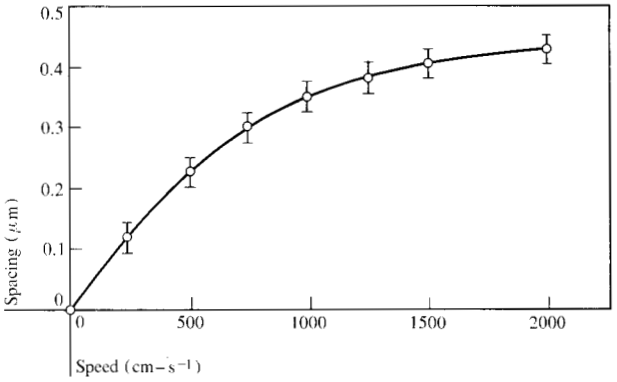

disk spacing is observed through the transparent slider, which is depicted schematically in Fig. 7(b), with photographs shown in Fig. 10. Finally, the transparent slider is flown on a functional surface and the slider-to-disk spacing is observed through the slider. Figure 11 shows the photographs for this condition.

The information from these three tests is then compared in order to correlate the glass disk testing with functional operation. Comparison of the first two tests, those run on the glass disk, shows that viewing the slider-to-disk spacing through the transparent slider does not distort the observation. This is illustrated in Fig. 12(a), showing good correlation between the observations made through the disk and those through the slid-

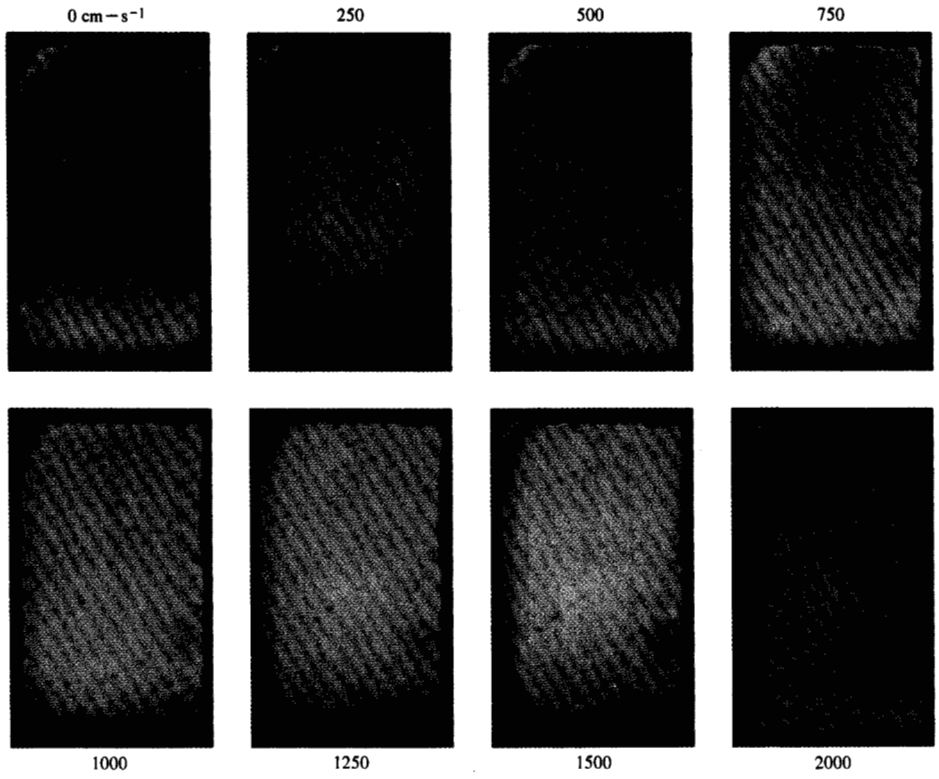

Figure 9 Color change vs speed for clear slider on glass disk, viewed through disk. Minimum slider-to-disk spacing is at top of each photograph.

Figure 10 Color change vs speed for clear slider on glass disk, viewed through slider. Minimum slider-to-disk spacing is at bottom of each photograph.

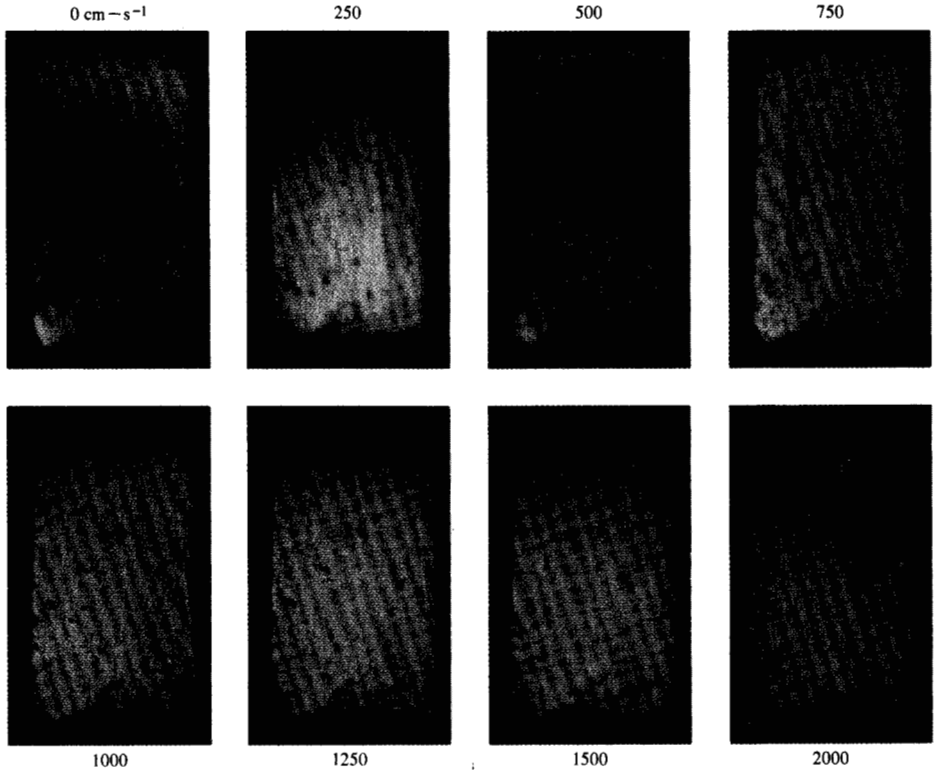

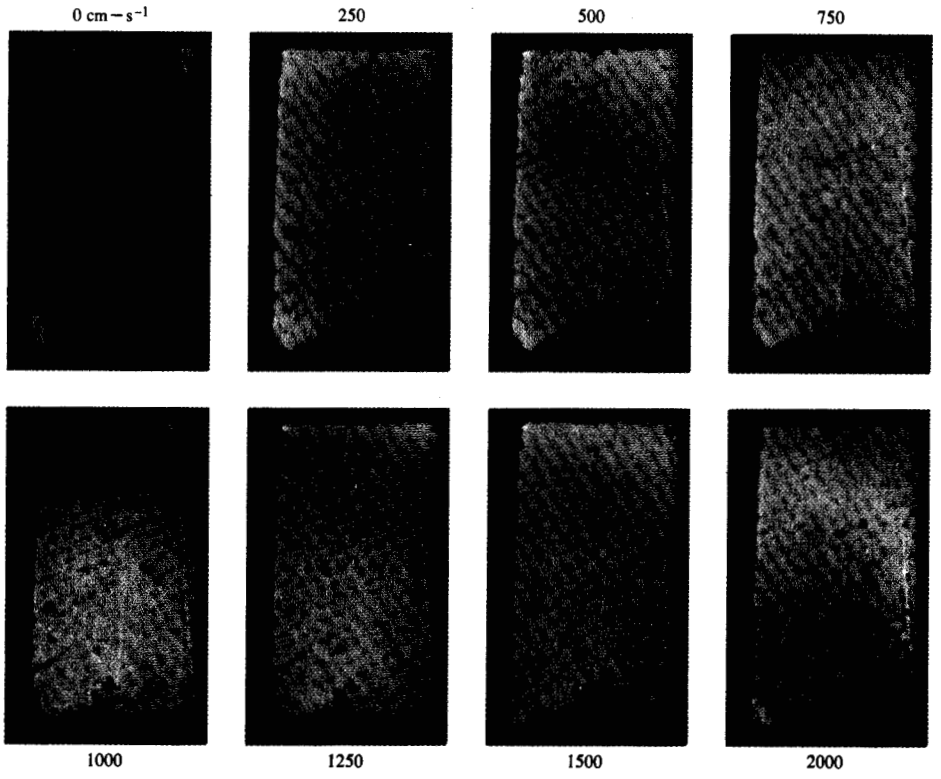

Figure 11 Color change vs speed for clear slider on magnetic disk, viewed through slider. Minimum slider-to-disk spacing is at bottom of each photograph.

Figure 12 Comparison of clear slider flown in various orientations: (a) slider-to-disk spacing on glass disk as viewed through disk and through slider; (b) slider-to-disk spacing as viewed through disk for a glass disk and as viewed through slider for a magnetic disk.

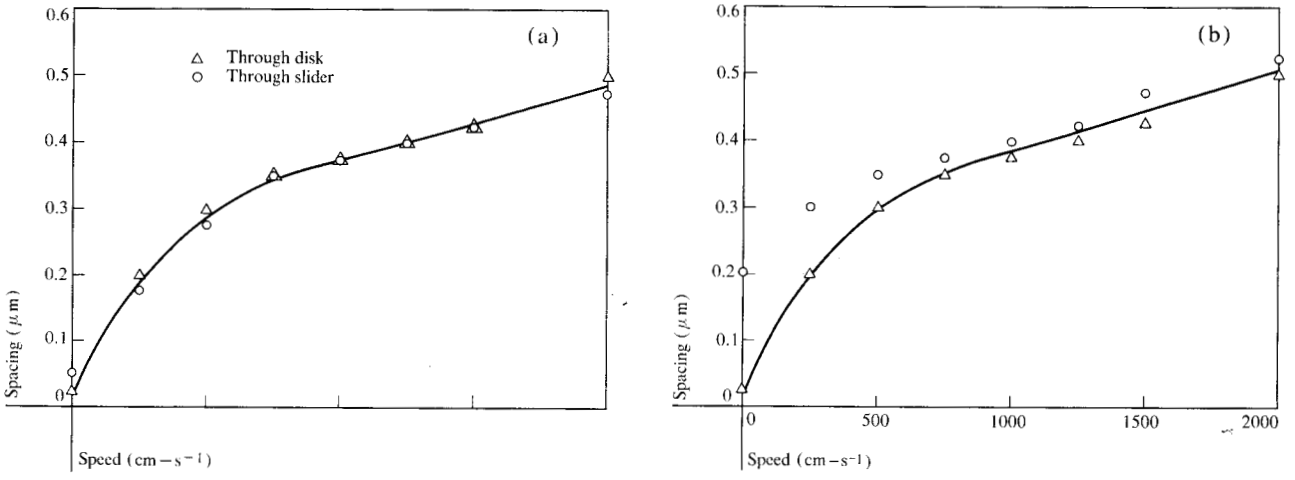

er. A comparison between the initial and final parts of the test demonstrates that the slider-to-disk spacing obtained for the glass disk is valid for predicting how a slider will fly on the functional surface. This is illustrated in Fig. 12(b), which shows the good correlation between the two tests at functional speeds. The initial difference in the slider-to-disk separation on the functional surface compared with that on the glass disk is attributed to the greater surface roughness of the functional surface. The slider is resting on asperities which hold it away from the reflecting surface of the disk. With increased speed this variation diminishes until all three conditions give

results within the 0.05-μm resolution provided by the technique.

Conclusions

White light interferometry has been successfully applied in the development of sliders for disk memory files. The important factors contributing to this success are the excellent resolution for film thicknesses below 1 μm, the full field-resolving capability for determining slider-to-disk spacing and slider attitude, and the simplicity of the equipment needed to create and monitor the white light interference pattern.

This technique could be applied to the measurement of any small movement that must be monitored with high resolution over the full field of observation. All that is required is an optically flat reference surface and a microscope with a vertical illuminator.

References

1. W. Gross, *Gas Film Lubrication*, John Wiley & Sons, New York 1962.
2. T. Tang, "Design and Analysis of Self-Acting Gas-Lubricated Slider Bearings for Noncontact Magnetic Recording," *ASME Publication 65-WA/MD-18*.
3. A. S. Hoagland, *Digital Magnetic Recording*, John Wiley & Sons, New York 1963.
4. V. M. Lieskovsky, "Optical Interference Techniques for Spacing Measurements in the 50 to 300 Microinch Range," presented at *MESUCORA 63 Congrés International*, Paris 1963.
5. M. Francon, *Optical Interferometry*, Academic Press, New York 1966, pp. 53–55.
6. R. A. Houston, *Physical Optics*, Blackie & Son Limited, London 1968, pp. 49–58.
7. R. W. Wood, *Physical Optics*, The MacMillan Company, New York 1934, pp. 188–194.
8. S. Tolansky, *Multiple-Beam Interferometry of Surfaces and Films*, Oxford University Press, London 1948, pp. 161–163.
9. F. A. Jenkins and H. E. White, *Fundamentals of Optics*, McGraw-Hill Book Company, Inc., New York 1957, pp. 250–251.

Received July 16, 1971

The authors are located at the IBM Systems Development Division Laboratory, San Jose, California 95114.